Publises or ance linewidth in FeCoSiB/Si/SiO₂/PMN-PT multiferroic neterostructures

Y. Gao, ^{1,a,b)} X. Wang, ^{1,b)} L. Xie, ¹ Z. Hu, ² Hwaider Lin, ¹ Z. Zhou, ³ T. Nan, ¹ X. Yang, ⁴ B. M. Howe, ² J. G. Jones, ² G. J. Brown, ² and N. X. Sun^{1,c)}

¹Department of Electrical and Computer Engineering, Northeastern University, Boston, Massachusetts, 02115, USA

²Materials and Manufacturing Directorate, Air Force Research Laboratory, Wright-Patterson Air Force Base, Dayton,

Ohio, 45433, USA

³Electronic Materials Research Laboratory, Key Laboratory of the Ministry of Education & International Center for

Dielectric Research, Xi'an Jiaotong University, Xi'an 710049, China

⁴School of Information and Electronics, Beijing Institute of Technology, Beijing, 100081, China

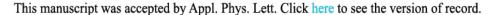
It has been challenging to achieve combined strong magnetoelectric coupling and narrow ferromagnetic resonance (FMR) linewidth in multiferroic heterostructures. Electric field induced large effective field of 175Oe and narrow FMR linewidth of 40Oe were observed in FeCoSiB/Si/SiO₂/PMN-PT heterostructures with substrate clamping effect minimized through removing the Si substrate. As a comparison, FeCoSiB/PMN-PT heterostructures with FeCoSiB film directly deposited on PMN-PT showed a comparable voltage induced effective magnetic field but a significantly larger FMR linewidth of 283Oe. These multiferroic heterostructures exhibiting combined giant magnetoelectric coupling and narrow ferromagnetic resonance linewidth offer great opportunities for integrated voltage tunable RF magnetic devices.

Multiferroic materials consisting of both magnetic property and ferroelectric performance have drawn a lot of attention due to the strong magnetoelectric (ME) coupling.¹⁻⁴ Recently, many multiferroic materials working in high frequency range have been reported, which give rise to a number of multiferroic RF devices, including filters, phase shifters, and integrated RF inductors.⁵⁻¹⁰ Moreover, by utilizing magnetic-piezoelectric heterostructures in which the electric field applied to the piezoelectric layer produces a mechanical deformation that couples to the magnetic film, and hence induces a magnetic anisotropy change, it is promising for one to develop electric field tunable RF devices due to strong ME coupling.¹¹⁻²⁴

a) Y. Gao is currently with Winchester Technologies, LLC.

b) Y. Gao and X. Wang contributed equally to this work.

c) Author to whom correspondence should be addressed. Electronic mail: n.sun@neu.edu.



AlPiffer

Publishing sses in order to maximize the electric field induced magnetic anisotropy. 25-53 By directly depositing of magnetic thin

films onto piezoelectric layers, Lou *et al.*²⁶ have reported a FeGaB/PMNPT multiferroic heterostructure showing a giant tunable resonance field of 330Oe. However a broad resonance linewidth of ~150Oe was detected, indicating a degraded magnetic performance due to large roughness from PMN-PT surface. As a comparison, they have also reported²⁷ a ME coupling at microwave frequencies in a layered structure of epoxy-bonded FeGaB/Si and PMN-PT slab, which exhibited a tunable resonance field of 30Oe while the linewidth was around 20Oe. However, due to the large thickness and stiffness of the Si substrate, the ME coupling strength is significantly reduced and far away from ideal, which is so-called substrate clamping effect. To summarize the pros and cons of above two typical heterostructures: the former one is maintaining a strong interface adhesion to get rid of substrate clamping effect, therefore, a relatively giant tunability can be obtained. However, the normally large roughness of piezoelectric layer causes poor magnetic film quality, which one can tell from broad linewidth; the latter one can always achieve high magnetic film quality hence narrow linewidth since small roughness Si is used as the substrate, but the induced magnetic anisotropy is quite limited due to substrate clamping effect. Moreover, many thin film heterostructures integrated on Si are also suffering from the substrate clamping effect. Moreover, many thin film heterostructures integrated on Si are also suffering from the substrate clamping effect meanwhile process. So it is still very challenging to demonstrate large ME coupling with minimized substrate clamping effect meanwhile maintaining narrow linewidth for multiferroic heterostructures and RF applications under a Si-friendly-circumstance.

In this work, FeCoSiB has been used due to its large magnetostriction constant (λ_s) and low saturation fields desired for low-cost integrated tunable microwave devices with narrow linewidth. The multiferroic composites FeCoSiB/Si/SiO₂/PMN-PT were prepared in which we induced DRIE (Deep Reactive-Ion Etching) MEMS process to remove Si substrate completely after FeCoSiB deposition over SOI (Si on insulator) wafer with in-film bias field of 2000e, then FeCoSiB (100nm) / Si (10 μ m) / SiO₂ (50nm) was epoxy bonded to 0.5mm (011) PMN-PT slab (H. C. Materials), with easy axis parallel and perpendicular to [01-1] direction respectively (Figure 1(a) and (b)). DRIE is a highly anisotropic etch process which can be utilized to remove Si from the backside of wafers to achieve very thin but still uniform carrier substrates. One can easily realize whatever thickness (nm~ μ m) needed for the substrate by controlling the thickness of buried SiO₂ layer and topmost Si layer of a SOI wafer. The substrate clamping effect is expected to be minimized by using this approach while the narrow linewidth can be maintained. Therefore, this feature provides an alternative route for preparing integrated multiferroic materials and fabricated Si-based tunable RF/micro-wave devices with very low loss. On the comparison, heterostructures FeCoSiB/PMN-PT were prepared by directly sputtering of FeCoSiB, under the same condition, onto PMN-PT slab with



cal parameters, with easy axis parallel to [01-1] direction, as schematically shown in Figure 1(c). Electric field induced

Publishing magnetic hysteresis loops were measured by vibration sample magnetometer (VSM, Lakeshore 7400). The field-

sweep FMR spectra under different electric fields were tested by electron spin resonance (ESR) spectrometer with a microwave cavity operating at TE_{102} mode and X-band (9.5GHz).

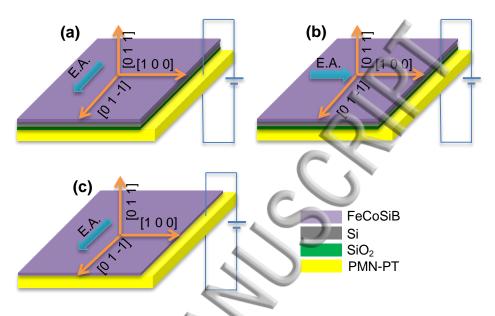


FIG. 1. Scheme showing the structure of the FeCoSiB/Si/SiO₂/PMN-PT laminate ((a) E.A.//[01-1], (b) E.A.//[100]) and the FeCoSiB/PMN-PT multiferroic heterostructure ((c) E.A.//[01-1]). The coordinate system shows the crystalline directions of the PMN-PT single crystal.

Compared to the widely used lead zirconate titanate ceramics which have a typical piezoelectric coefficient d_{31} of ~-200pC/N, PMN-PT single crystals used in this work with 28-32% PT exhibit much larger in-plane piezoelectric coefficients of d_{31} of ~-1800pC/N and d_{32} of ~900pC/N for <011> poling. Given that the FeCoSiB films are very thin compared to the PMN-PT substrates for both kinds of laminates, they would experience the same strain states as the PMN-PT under electric field. Therefore, large in-plane biaxial strain is expected within the FeCoSiB film, allowing voltage control of magnetism by strain-mediated ME coupling. The electric field induced change in the in-plane magnetic anisotropy field ΔH_{eff} can be calculated by the piezoelectric and inverse magnetoelastic equations

$$DH_{eff} = 3/_{S} d_{eff} EY/M_{S} \tag{1}$$

where λ_S is the saturation magnetostriction constant, Y the Young's modulus of the magnetic film, d_{eff} the effective piezoelectric coefficient, E the applied electric field, and M_S the saturation magnetization. And d_{eff} can be expressed as

$$d_{eff} = \frac{vd_{32} + d_{31}}{1 - v^2} - \frac{vd_{31} + d_{32}}{1 - v^2} = \frac{d_{31} - d_{32}}{1 + v}$$
 (2)

where *v* is the Poisson ratio of the magnetic film. According to Equation (2), it is concluded that the giant anisotropic tric coefficients of the PMN-PT provide great opportunities for generating a large in-plane magnetic anisotropic field and hence a large frequency tunability in RF applications.

Electric field induced change in magnetic hysteresis loops of the FeCoSiB/PMN-PT multiferroic heterostructure along [01-1] direction of the PMN-PT single crystal is shown in Figure 2(a). The remnant magnetization ratio shows a remarkable change when the electric field was varied from 0 to +8kV/cm. A low anisotropy field is achieved at zero electric field while electric field of +8kV/cm corresponds to a much higher anisotropy field. One can also see a relatively high coercive field of 25~40Oe caused by the large roughness (~10nm) of the PMNPT surface. Compared to this, Figure 2(b) gives the magnetic hysteresis loops of the FeCoSiB/Si/SiO₂/PMN-PT laminate along the same direction at various electric fields. A Clear and similar trend of anisotropy field change is also observed. At the same time, a much lower coercive field of ~10Oe is obtained, implying a low loss and high quality of the magnetic film attributed to the much smaller roughness (~0.2nm) of the Si surface.

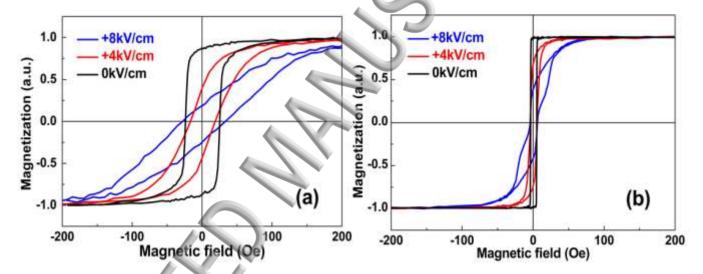


FIG. 2. Magnetic hysteresis loops of (a) the FeCoSiB/PMN-PT multiferroic heterostructure and (b) the FeCoSiB/Si/SiO₂/PMN-PT laminate at various electric fields along the [01-1] direction.

The field-sweep FMR spectra of the FeCoSiB/PMN-PT multiferroic composites along [01-1] under different electric fields are represented in Figure 3(a). A large shift of the FMR field from 615Oe to 780Oe can be observed with the applied electric field of +8kV/cm. A butterfly-like curve of the effective FMR field (H_{eff}) as a function of electric field is exhibited in Figure 3(b) with a maximum tunability of 180Oe. This again demonstrates the control of the effective magnetic field by electric field via strain mediated mechanism due to the piezoelectric effect. However, a linewidth over 283Oe is shown in Figure 3(a), indicating a large magnetic loss of the magnetic film. In terms of FeCoSiB/Si/SiO₂/PMN-PT sample, on the comparison, Figure 3(c) illustrates the electric field dependence of the effective magnetic anisotropy fields from the ME coupling along the same direction (E.A.//[01-1]). The large shift of the effective FMR field from 570Oe to 730Oe with the



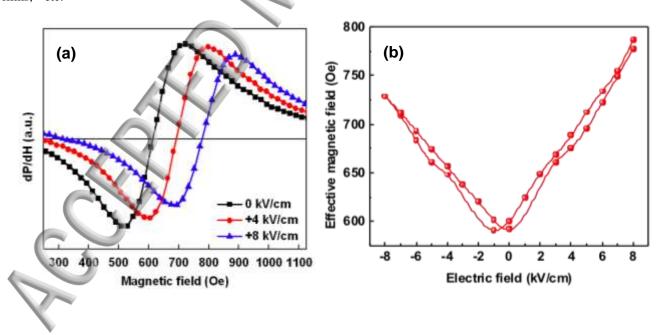
Publishing in this case (Figure 3(d)) shows a maximum tunability of 1750e, which is quite close to the value measured to the

FeCoSiB/PMN-PT laminate, indicating an effective minimization of the substrate clamping effect. At the same time, according to Figure 3(c), a narrow linewidth of ~40Oe is achieved, which means the magnetic layer is holding a low tangent loss and a high quality factor. This is also in good agreement with the results of the magnetic hysteresis loops as shown in Figure 2(b).

As seen in all the curves under different electric fields in Figure 3(c), there is a second FMR signal located on the lower field sides of the main peak, which is a standing spin wave described as

$$H_n = H_0 - 2\pi^2 A n^2 / (M_S d^2) \tag{3}$$

where H_n is the corresponding field for exciting a particular spin-wave mode, n the volume spin wave mode number, A the exchange constant, related to the exchange coupling, and d the thickness of the magnetic film.⁵⁴ The uniform processing mode corresponds to the case of n=0. The standing spin-wave modes observed here are most likely the case of n=1, which are the first modes to the lower field side of the main peak. The standing spin wave is due to the surface anisotropy of magnetic film.^{55, 56} A difference of 130Oe between H_0 and H_1 can be observed in Figure 3(c). The FeCoSiB film tested exhibits a $4\pi M_S$ of 1.4T and the thickness d is 100nm. The exchange constant A, therefore, calculated from Equation (3) is 0.73×10^{-6} erg/cm, which is comparable to the exchange constants of other magnetic materials such as permalloy,⁵⁷ FeAIN,⁵⁴ and Co-based films,⁵⁸ etc.



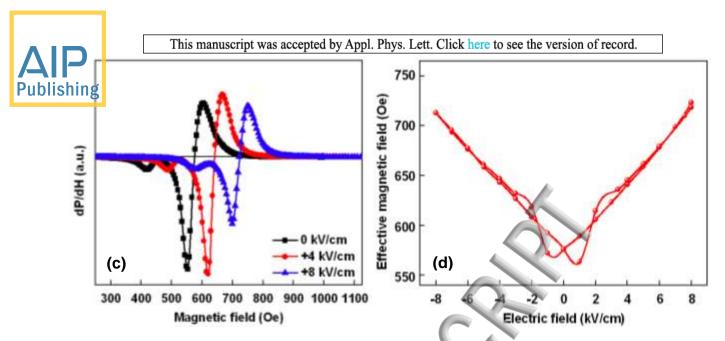


FIG. 3. (a) FMR spectra of the FeCoSiB/PMN-PT multiferroic heterostructure at various electric fields, and (b) Effective FMR fields as a function of electric field with the external magnetic fields along [01-1] direction of PMN-PT; (c) FMR spectra of the FeCoSiB/Si/SiO₂/PMN-PT laminate at various electric fields, and (d) Effective FMR fields as a function of electric field with the external magnetic fields along E.A.// [01-1] direction of PMN-PT.

Figure 4(a) gives the change of FMR field along E.A.//[100] directions at various electric fields. As illustrated, the ferromagnetic resonance field shifts downwards by 90Qe under an electric field of +8kV/cm with a linewidth of ~50Qe. Correspondingly, the butterfly curves is exhibited in Figure 4(b), implying a maximum magnetism tunability of ~100Qe. On the contrary, a different electric field dependency is displayed when the FeCoSiB/Si/SiO₂/PMN-PT heterostructure was tested with external magnetic field along H.A.//[01-1] direction. This is reflected by the opposite trend of the effective magnetic field shift and butterfly-like curve versus electric field, as shown in Figure 4(c) and (d). The resonance field shifts upwards from 650Qe at 0kV/cm to 750Qe at +8kV/cm and a maximum tunability of 100Qe can be observed. A narrow linewidth of ~60Qe is obtained as well. It is notable that the absolute values of the change of magnetic anisotropy field along [100] and [01-1] directions are identical, which is consistent with the descriptions of Equation (1) and (2).

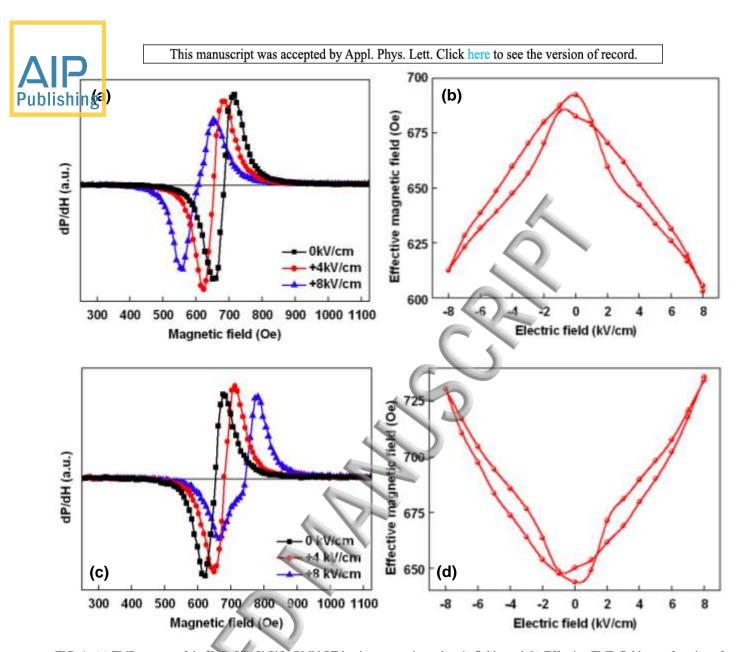


FIG. 4. (a) FMR spectra of the FeCoSiB/Si/SiO₂/PMN-PT laminate at various electric fields, and (b) Effective FMR fields as a function of electric field with the external magnetic fields along E.A.// [100] direction of PMN-PT; (c) FMR spectra of the FeCoSiB/Si/SiO₂/PMN-PT laminate at various electric fields, and (d) Effective FMR fields as a function of electric field with the external magnetic fields along H.A.// [01-1] direction of PMN-PT.

In summary, by utilizing DRIE process to minimize the substrate clamping effect, we have demonstrated a large magnetism tunability of 175Oe through electric field induced, strain mediated ME coupling in FeCoSiB/Si/SiO₂/PMN-PT multiferroic laminates. Meanwhile, the FMR linewidth of the FeCoSiB film, which is critical parameter for microwave magnetic materials, stays under 50Oe. The ratio between the total tunable magnetic field and the FMR linewidth is as high as 450%, which is much higher compared to the direct deposited FeCoSiB/PMN-PT heterostructures with a ratio of 64% (180Oe/283.03Oe). This indicates an excellent figure of merit for low loss microwave devices. Since the SOI substrates (Si/SiO₂/Si) used in this work have 10 μm thick topmost Si layer, it is worth mentioning that better ME coupling performance can be expected in FM/SiO₂/PE heterostructures where regular SiO₂/Si substrates are used. Therefore, this work provides a

This manuscript was accepted by Appl. Phys. Lett. Click here to see the version of record.

Publishing lent microwave performances. For instance, RF magnetoelectric inductors using DRIE followed by PMN-PT bonding process has been reported with a giant voltage tunable inductance of >100% and a high quality factor. ^{23, 59}

The work was financially supported by W. M. Keck Foundation, National Science Foundation (NSF) awards 1160504 and 1533484, and performed in part at the Center for Nanoscale Systems (CNS), a member of the National Nanotechnology Infrastructure Network (NNIN), which is supported by the National Science Foundation under NSF award no. ECS-0335765. CNS is part of Harvard University.

⁸Y. Gao, S. Zare, X. Yang, T. Nan, Z. Zhou, M. Onabajo, M. Liu, A. Aronow, K. Mahalingam, B. Howe, G. Brown, and N. Sun, IEEE Trans. Electron Devices. 61, 1470 (2014).

⁹X. Yang, Z. Zhou, T. Nan, Y. Gao, G. Yang, M. Liu, and N. Sun, Journal of Materials Chemistry C 4, 234 (2016).

¹⁰X. Yang, Y. Gao, J. Wu, Z. Zhou, s. Beguhn, T. Nan, and N. Sun, IEEE Microwave and Wireless Components Letters 24, 191 (2014).

¹¹G. Subramanyam, M. Cole, N. Sun, T. Kalkur, N. Sbrockey, G. Tompa, X. Guo, C. Chen, S. Alpay, G. Rossetti, K. Dayal, L. Chen, and D. Schlom, J. Appl. Phys. 114, 191301 (2013).

¹W. Eerenstein, N. D. Mathur, and J. F. Scott, Nature 442, 759 (2006)

²N. Spaldin and R. Ramesh, MRS Bull 33, 1047 (2008).

³C. Nan, M. I. Bichurin, S. Dong, D. Viehland, and G. Srinivasan, J. Appl. Phys. 103, 031101 (2008).

⁴S. Dong, J. Zhai, J. Li, and D. Viehland, Appl. Phys. Lett. 89, 252904 (2006).

⁵X. Yang, Y. Gao, J. Wu, S. Beguhn, T. Nan, Z. Zhou, M. Liu, and N. Sun, IEEE Trans. Magn 49, 5485 (2013).

⁶Y. Gao, S. Zare, X. Yang, T. Nan, Z. Zhou, M. Onabajo, K. O'Brien, U. Jalan, M. EI-tatani, P. Fisher, M. Liu, A. Aronow, K. Mahalingam, B. Howe, G. Brown, and N. Sun, J. Appl. Phys. 115, 17E714 (2014).

⁷X. Yang, J. Wu, Y. Gao, T. Nan, Z. Zhou, S. Beguhn, M. Liu, and N. Sun, IEEE Trans. Magn 49, 3882 (2013).

¹²N. Sun and G. Srinivasan, SPIN 2, 1240004 (2012).

¹³M. Liu and N. Sun, Philos. Trans. R. Soc., A 372, 20120439 (2014).

¹⁴A. Ustinov, G. Srinivasan, and B. Kalinikos, Appl. Phys. Lett. 90, 031913 (2007).

¹⁵J. Das, Y. Song, N. Mo, P. Krivosik, and C. Patton, Adv. Mater. 21, 2045 (2009).

¹⁶J. Hu, Z. Li, L. Chen, and C. Nan, Nat. Commun. 2, 553 (2011).

¹⁷T. Nan, Z. Zhou, J. Lou, M. Liu, X. Yang, Y. Gao, S. Rand, and N. Sun, Appl. Phys. Lett. 100, 132409 (2012).

This manuscript was accepted by Appl. Phys. Lett. Click here to see the version of record.



E. Tsymbal, Nat. Mater. 11, 12 (2011)

Publishing Nan, Y. Hui, M. Rinaldi, and N. Sun, Sci. Rep. 3, 1985 (2013).

²⁰J. Zhai, Z. Xing, S. Dong, J. Li, and D. Viehland, Appl. Phys. Lett. 88, 062510 (2006).

²¹H. Lin, J. Lou, Y. Gao, R. Hasegawa, M. Liu, B. Howe, J. Jones, G. Brown, and N. Sun, IEEE Trans. Magn. 51, 1 (2015).

²²X. Yang, J. Wu, S. Beguhn, T. Nan, Y. Gao, Z. Zhou, and N. Sun, IEEE Microwave and Wireless Components Letters 23, 184 (2013).

²³Y. Gao, S. Zare, M. Onabajo, M. Li, Z. Zhou, T. Nan, X. Yang, M. Liu, K. Mahalingam, B. Howe, G. Brown, and N. Sun, *Microwave Symposium (IMS)* 2014 IEEE MTT-S International, Florida, USA, June 2014.

²⁴H. Lin, J. Wu, X. Yang, Z. Hu, T. Nan, S. Emori, Y. Gao, R. Guo, X. Wang, and N. Sun, *Microwave Symposium (IMS)* 2015 IEEE MTT-S International, Arizona, USA, June 2015.

²⁵C. A. F. Vaz, J. Hoffman, C. H. Ahn, and R. Ramesh, Adv. Mater. 22, 2900 (2010).

²⁶J. Lou, M. Liu, D. Reed, Y. Ren, and N. Sun, Adv. Mater. 21, 4711 (2009).

²⁷J. Lou, D. Reed, C. Pettiford, M. Liu, P. Han, S. Dong, and N. Sun, Appl. Phys. Lett. 92, 262502 (2008).

²⁸H. Greve, E. Woltermann, H. J. Quenzer, B. Wagner, and E. Quandt, Appl. Phys. Lett. 96, 182501 (2010).

²⁹Z. Zhou, T. Nan, Y. Gao, X. Yang, S. Beguhn, M. Li, Y. Lu, J. Wang, M. Liu, K. Mahalingam, B. M. Howe, G. J. Brown, and N. Sun, App. Phys. Lett. 103, 232906 (2013).

³⁰G. Srinivasan, in Annual Review of Materials Research (2010).

³¹J. H. Lee, L. Fang, E. Vlahos, X. L. Ke, Y.W. Jung, L. F. Kourkoutis, J. W. Kim, P. J. Ryan, T. Heeg, M. Roeckerath, V. Goian, M. Bernhagen, R. Uecker, P. C. Hammel, K. M. Rabe, S. Kamba, J. Schubert, J. W. Freeland, D. A. Muller, C. J. Fennie, P. Schiffer, V. Gopalan, E. Johnston-Halperin, and D. G. Schlom, Nature (London) 476, 114 (2011).

³²M. Liu, O. Obi, J. Lou, Y. Chen, Z. Cai, S. Stoute, M. Espanol, M. Lew, X. Situ, K. Ziemer, V. Harris, and N. Sun, Adv. Funct. Mater. 19, 1826 (2009).

³³S. Li, Q. Xue, H. Du, J. Xu, Q. Li, Z. Shi, X. Gao, M. Liu, T. Nan, Z. Hu, N. Sun, and W. Shao, J. Appl. Phys. 117, 17D702 (2015).

³⁴Z. Zhou, S. Zhao, Y. Gao, X. Wang, T. Nan, N. Sun, X. Yang, and M. Liu, Sci. Rep. 6, 20450 (2016).

³⁵Y. Chen, J. Wang, M. Liu, J. Lou, N. Sun, C. Vittoria, and V. Harris, Appl. Phys. Lett. 93, 112502 (2008).

³⁶T. Wu, A. Bur, K. Wong, J. Leon Hockel, C.-J. Hsu, H. K. D. Kim, K. L. Wang, and G. P. Carman, J. Appl. Phys. 109, 07D732 (2011).



D. A. Filippov, G. Srinivasan, and A. Gupta, J. Phys. Condens. Matter 20, 425206 (2008).

Publishing M. Petrov, G. Srinivasan, M. I. Bichurin, and A. Gupta, Phys. Rev. B 75, 224407 (2007).

- ³⁹Z. Zhou, T. Nan, M. Liu, Y. Gao, X. Yang, M. Li, N. Sun, and G. Brown, Sci. Rep. 4, 3688 (2014).
- ⁴⁰T. Nan, Z. Zhou, M. Liu, X. Yang, Y. Gao, B. Assaf, H. Lin, S. Velu, X. Wang, H. Luo, J. Chen, S. Akhtar, E. Hu, R. Rajiv, K. Krishnan, S. Sreedhar, D. Heiman, B. Howe, G. Brown, and N. Sun, Sci. Rep. 4, 3688 (2014).
 - ⁴¹S. Zhang, J. Luo, W. Hackenberger, and T. R. Shrout, J. Appl. Phys. 104, 064106 (2008).
- ⁴²Z. Zhou, X. Zhang, T. Xie, T. Nan, Y. Gao, H. Lin, X. He, P. Qiu, N. Sun, and D. Sun, Appl. Phys. Lett. 104, 012905 (2014).
 - ⁴³P. Finkel, C. J. Murphy, J. Stace, K. Bussmann, A. Heitmann, and A. Amin, Appl. Phys. Lett. 102, 182903 (2013).
 - ⁴⁴Z. Hu, T. Nan, X. Wang, M. Staruch, Y. Gao, P. Finkel, and N. Sun, Appl. Phys. Lett. 106, 022901 (2015).
 - ⁴⁵E. Sun, S. Zhang, J. Luo, T. R. Shrout, and W. Cao, Appl. Phys. Lett. 97, 032902 (2010).
 - ⁴⁶T. Nan, Z. Zhou, J. Lou, M. Liu, X. Yang, Y. Gao, S. Rand and N. Sun, Appl. Phys. Lett. 100, 132409 (2012).
 - ⁴⁷Y. K. Fetisov and G. Srinivasan, Appl. Phys. Lett. 88, 143503 (2006).
- ⁴⁸Z. Zhou, O. Obi, S. Beguhn, T. Nan, J. Lou, X. Wang, Y. Gao, M. Li, S. Rand, N. Sun, G. Esteves, J. Jones, K. Mahalingam, M. Liu, and G. Brown, J. Mater. Sci: Mater. Electron. 25, 1188 (2014).
- ⁴⁹Y. H. Chu, L. W. Martin, M. B. Holcomb, M. Gajek, S. J. Han, Q. He, N. Balke, C. H. Yang, D. Lee, W. Hu, Q. Zhan, P. L. Yang, A. Fraile-Rodriguez, A. Scholl, S. X. Wang, and R. Ramesh, Nature Mater. 7, 678 (2008).
- ⁵⁰T. Nan, S. Emori, B. Peng, X. Wang, Z. Hu, L. Xie, Y. Gao, H. Lin, J. Jiao, H. Luo, D. Budil, J. Jones, B. Howe, G. Brown, M. Liu, and N. Sun, Appl. Phys. Lett. 108, 012406 (2016).
- ⁵¹X. He, Y. Wang, N. Wu, A. N. Caruso, E. Vescovo, K. D. Belashchenko, P. A. Dowben, and C. Binek, Nature Mater. 9, 579 (2010).
 - ⁵²M. Bibes and A. Barthelemy, Nature Mater. 7, 425 (2008).
 - ⁵³N. A. Spaldin, S. W. Cheong, and R. Ramesh, Phys. Today 63, 38 (2010).
 - ⁵⁴K. Rook and J. O. Artman, IEEE Trans. Magn., 27, 5450 (1991).
 - ⁵⁵B. Hillebrands, Phys. Rev. B, 41, 530 (1990).
 - ⁵⁶X. Xing, M. Liu, S. Li, O. Obi, J. Lou, Z. Zhou, B. Chen, and N. Sun, IEEE Trans. Magn., 47, 3104 (2011).
 - ⁵⁷ A. Z. Maksymowicz, J. S. S. Whiting, M. L. Watson, and A. Chambers, Thin Solid Films. 197, 287 (1991).
 - ⁵⁸O. Gaier, Ph. D. thesis, Technical University of Kaiserslautern, 2009.
 - ⁵⁹Y. Gao, Ph.D. thesis, Northeastern University, Boston, 2015.

